Chemical Structure of Soil Organic Matter in Slickspots as Investigated by Advanced Solid-State NMR

Jingdong Mao,[1] Antonio J. Palazzo,[2] Dan C. Olk,[3] C. Edward Clapp,[4] Nicola Senesi,[5] Terry L. Bashore,[6] and Xiaoyan Cao[1]

Abstract: Slickspot soils are saline, and knowledge of their humic chemistry would contribute to our limited understanding how salinity affects soil C and N stocks. We characterized humic acids (HA) from slickspot soils with solid-state ^{13}C nuclear magnetic resonance (NMR). Expanding on previous use of cross polarization/magic angle spinning (CP/MAS) NMR, we used direct polarization (DP) and yet more advanced spectral editing techniques to identify specific functional groups, detect the connectivities of different functional groups, and selectively observe fused ring carbons. A series of soil HA was extracted from soil layers having different physical properties: silt texture, vesicular structure, and clay texture. They were compared with HA from corresponding depths in soils adjacent to the slickspots. All HA consisted of five main structural components: aliphatic chains, peptides, sugar rings, lignin residues, and aromatics/olefinics. For all soils, except one outside slickspots, the HA from the vesicular and clay layers contained less nonpolar alkyls and more aromatics than those from surface silt layers, but their spectral proportions differed when the ^{13}C NMR was performed using CP/MAS instead of DP. Humic acids from the surface layers inside the slickspots had lower aromaticity than those from outside the slickspots. Advanced spectral editing techniques allowed for the selection of nonprotonated carbons and mobile groups, alkyls, CH, and CH_2 groups, which would otherwise be buried in the heavily overlapped spectrum. They provided more structural information than was obtained by routine ^{13}C CP/MAS or DP.

Key words: Humic acids, nuclear magnetic resonance, chemical structure, slickspot soils, soil layers.

(*Soil Sci* 2010;175: 329–338)

Slickspots, small-scale depressions where water collects, are common features on sodic soils. Slickspots exist in many arid and semiarid areas. For example, in the lower Malheaur River Valley in southeastern Oregon and the Boise and Payette River Valleys in Idaho, more than 55,000 ha of irrigated lands contain small areas of slickspot soils (Rasmussen et al., 1972; Reid et al., 1993). These soils are salt affected and unproductive. Previous studies found that slickspot soils had higher salt content, pH, sodium adsorption ratio, and electrical conductivity than adjacent soils outside the slickspots (Fisher et al., 1996). Soil contents of P, K, C, and N were less for slickspot soils than outside soils. Palazzo et al. (2008) found greater concentrations of soil Na in slickspot soils compared with outside the slickspots and also greater electrical conductivity values with depth; this may indicate water storage inside the slickspots because of the deep B-clay horizon. Above the subsoil clay horizon is a layer having vesicular structure, which consists of pores unconnected to each other. Vesicular crusts are common in silty surface soils of the Great Basin, most notably in shrub interspaces where organic contents are low (Fisher et al., 1996). There may be lateral movement of water and salts from adjacent soil into slickspots with little or no movement of water and salts downward in the slickspot (Lewis and White, 1964). This pattern of moisture movement would help explain why Na and other salts have not been leached out of the slickspot.

In contrast to these inorganic soil components, the organic components of slickspot soils have not been studied in detail. Even more broadly, effects of salinity on soil C stocks have received little attention. Elevated salinity increased soil C mineralization during one controlled incubation, perhaps by either increased dispersion of soil aggregates or hydrolysis of soil organic matter (SOM) (Wong et al., 2008). Changes in soil microbial populations caused by salinity might alter soil C fluxes in other ways (Luna-Guido et al., 2001; Li et al., 2006). Nelson et al. (1996) found increased salinity, decreased C mineralization of incorporated plant litter during controlled incubation, but neither plant- nor soil-derived microbial biomass was greatly affected. The chemical nature of SOM in saline soils has received virtually no attention.

Various methods have been used to study the chemical structures of SOM. Among them, solid-state ^{13}C nuclear magnetic resonance (NMR) has been considered one of the most suitable ones (Preston, 1996; Nanny et al., 1997, Mathers et al., 2000; and Hatcher et al., 2001). Since the early 1980s, considerable knowledge on soil C forms has been gained through NMR by using the cross-polarization/magic angle spinning (CP/MAS) approach (Preston, 1996). In this approach, sensitivity is substantially improved through the transfer of magnetization from the abundant ^{1}H to dilute ^{13}C spins by CP (Pines et al.,1973). Yet CP-MAS is not accurate in estimating the spectral proportions of C because this technique is not fully quantitative. It has reduced efficiency for nonprotonated carbons, mobile components, and regions having short proton rotating-frame spin-lattice relaxation time ($T_{1\rho}{}^{H}$). Also the CP/MAS spectra of SOM have broad overlapping peaks, and it is difficult to make specific assignments. Direct polarization (DP)/MAS is a quantitative technique because it involves only DP, and the problems associated with reduced CP can be avoided. The problem with DP is its long acquisition time. Similar to ^{13}C CP/MAS, ^{13}C DP/MAS spectra of SOM can also have broad peaks.

To obtain specific functional groups from the broad SOM spectra, advanced selective spectral-editing techniques were developed in recent years (Mao et al., 2007a; 2007b). Combining other advanced techniques, we developed a protocol for systematically characterizing complex natural organic matter in

[1]Department of Chemistry and Biochemistry, Old Dominion University, Norfolk, VA 23529. Dr. Jingdong Mao is corresponding author. E-mail: jmao@odu.edu
[2]USACOE, Cold Regions Research and Engineering Laboratory, Hanover, NH.
[3]USDA-ARS, National Laboratory for Agriculture and the Environment, Ames, IA.
[4]USDA-ARS & Department of Soil, Water, and Climate, University of Minnesota, St Paul, MN.
[5]Dipartimento di Biologia e Chimica Agroforestale e Ambientale, Universita di Bari, Bari, Italy.
[6]Airspace, Ranges, and Air Field Operations Division, HQ Air Combat Command, Langley AFB, VA.
Received November 21, 2009.
Accepted for publication May 21, 2010.

ISSN: 0038-075X
DOI: 10.1097/SS.0b013e3181e93d23

plant, soil, water, sediment, manure, sludge, and meteorite samples. This protocol includes identification of specific functional groups, detection of connectivities, and examination of domains and heterogeneity (Mao et al., 2007a; Mao and Schmidt-Rohr, 2006). Traditional ^{13}C-NMR spectra for complex organic matter can identify only about 10 types of chemical groups because routine solid-state ^{13}C-NMR spectra consist of broad and heavily overlapped bands in which functional groups cannot be clearly distinguished. With our new NMR techniques, we have clearly identified more than 40 different moieties. In addition, we can use ^{1}H spin diffusion to detect domains or heterogeneities on a scale of 1 to 50 nm.

A humic acid (HA) fraction that was extracted from three depths for soils inside and outside slickspots in the Juniper Butte Range was previously analyzed by ^{13}C CP/MAS NMR (Palazzo et al., 2008). In the present study, we used ^{13}C DP/MAS, advanced spectral-editing techniques, and two-dimensional ^{1}H-^{13}C heteronuclear correlation NMR (2D HETCOR) to analyze the same HA samples that were analyzed by Palazzo et al. (2008). It is our goal to address the following four questions. First, what are the advantages of quantitative and advanced solid-state NMR techniques over routine ^{13}C CP/MAS? Second, what are the primary structural units of HA from the slickspot soils? Third, how do the chemical structures of HA vary with soil depth? Finally, how do the chemical structures of HA vary within and outside slickspots?

MATERIALS AND METHODS

Environmental Setting and Sampling

Soil samples were collected on the U.S. Air Force Juniper Butte Range, Owyhee County, Idaho. Juniper Butte Range is located 75 km southeast of Bruneau and 77 km southwest of Twin Falls, Idaho, with an area of ca. 4,877 ha. Soils were sampled from a 45-ha area in the southeast corner of the range.

Slickspots are unmapped inclusions with the Arbidge-Chilcott silt loams, which are Abruptic Durargids (Sandoval et al., 1959; Harkness 1998). They have been discussed but not formally described pedologically (Harkness, 1998; Fisher, 1996). Slickspots have a puddled, crusted, or smooth surface with an excess of exchangeable sodium (Harkness 1998). Drainage swales commonly bisect the landscape, and some slickspots have the seasonal ability to pond water. Slickspot soils are silt to clay in texture and mostly devoid of vegetation. Below the surface layer is the vesicular layer that is partially impermeable to water infiltration and can cause water ponding. The profile below the vesicular layer is dominated by the subsoil clay layer (Lewis et al., 1959; Fisher et al.,1996).

Soil was obtained from inside and outside two slickspots at two separate locations in the Juniper Butte Range. They are numbered 4 and 5 and are representative of several other slickspots in the Juniper Butte Range. Previous work on Idaho slickspots did not mention substantial variability among slickspots (Lewis and White, 1964), so we will presume that analysis of these two sites enables to some degree a general discussion of slickspot soil properties. Samples were collected at three different layers within the soil profile: silt (0–2.5 cm), vesicular (2.5–3.5 cm), and clay (3.5–15 cm). Samples collected outside the slickspots were within 3 m of the slickspots to a depth of 15 cm. No vesicular layer was found outside the slickspots for both sites. Soils from each layer were air-dried and ground to pass through a 2-mm mesh screen before analysis. Selected properties of soil within or adjacent to nine slickspots in this area are shown in Table 1. The measurements were based on the methods described by Jones (1999).

TABLE 1. Selected Properties of Soil Within or Adjacent to Nine Slickspots

Parameter*	Inside Slickspot	Outside Slickspot	*P*
Total C, g/kg	6.2 ± 0.5	10.3 ± 1.8	0.017
Total N, g/kg	0.6 ± 0.0	0.9 ± 0.1	0.077
pH	7.6 ± 0.1	7.0 ± 0.1	<0.001
Electrical conductivity, dS/m (ln[b])	2.8 ± 0.3	0.6 ± 0.1	<0.001
Na adsorption ratio, ln	16.9 ± 2.7	7.3 ± 2.5	0.034
Extractable K, mg/kg	164 ± 13	289 ± 18	<0.001
Extractable P	11.3 ± 1	15.7 ± 2.8	0.48

*Note that the data are based on the averages across nine slickspot soils.

The soil samples will henceforth be named by three-part abbreviations that list in order the sampling site, whether the soil is inside or outside a slickspot, and depth. Therefore, from top to bottom, at Site 4, the samples inside the slickspots are 4-inside-silt (0–2.5 cm), 4-inside-vesicular (2.5–3.5 cm), and 4-inside-clay (3.5–15 cm). The corresponding samples outside the slickspots at Site 4 are 4-outside-silt and 4-outside-clay. At Site 5, ranging from top to bottom, the samples inside the slickspots are 5-inside-silt (0–2.5 cm), 5-inside-vesicular (2.5–3.5 cm), and 5-inside-clay (3.5–15 cm). The corresponding two samples outside the slickspots at Site 5 are 5-outside-silt (0–2.5 cm) and 5-outside-clay (3.5–15 cm).

Extraction of HA Fraction

To obtain a purely organic sample for further analysis, an HA fraction was extracted from the soil samples using a modified version of the International Humic Substances Society procedure (Swift, 1996). Extraction was carried out using 0.5 *M* NaOH under N_2 gas. The extract was membrane filtered (0.2-mm pore size), the filtrate was adjusted to pH 1 (6 *M* HCl), and the precipitated HA was centrifuged, dialyzed, and freeze dried (Palazzo et al., 2008).

NMR Spectroscopy

All NMR experiments were performed using a Bruker DSX400 spectrometer at 100 MHz for ^{13}C. All experiments were performed with 7-mm sample rotors except for the high-speed experiments at 14 kHz, which were run with 4-mm rotors.

High-Speed Quantitative ^{13}C DP/MAS NMR

Quantitative ^{13}C DP/MAS experiments were run at a spinning speed of 14 kHz. The 90-degree ^{13}C pulse length was 4 μsec. Recycle delays were tested by the CP/T1-TOSS technique to make sure that all carbon sites are fully relaxed (Mao et al., 2000). The numbers of scans and recycle delays are listed in the figure captions. To highlight mobile groups, ^{13}C DP/MAS with a short recycle delay of 1.5 sec was used.

^{13}C CP/TOSS and ^{13}C CP/TOSS Plus Dipolar Dephasing

Qualitative composition information was obtained with good sensitivity by ^{13}C CP/total sideband suppression (CP/TOSS) NMR experiments at a spinning speed of 6.5 kHz and a CP time of 1 msec, with ^{1}H 90-degree pulse length of 4 μsec. Four-pulse TOSS (Dixon, 1982) was used before detection, and two-pulse phase-modulated decoupling was applied for optimum resolution.

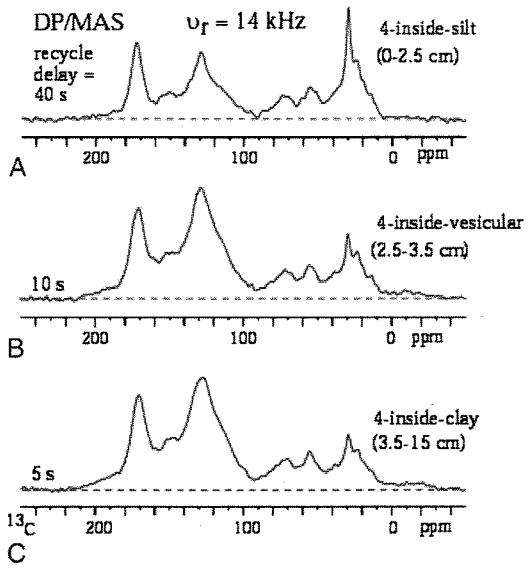

FIG. 1. Quantitative DP/MAS ^{13}C NMR spectra of (A) 4-inside-silt HA with a recycle delay of 40 sec and 1,792 scans, (B) 4-inside-vesicular HA with a recycle delay of 10 sec and 1,440 scans, (C) 4-inside-clay HA with a recycle delay of 5 sec and 8,192 scans. Spinning frequency was 14 kHz.

The ^{13}C CP/TOSS combined with 40-μsec dipolar dephasing experiment was also used to generate a subspectrum with nonprotonated carbons and mobile groups such as CH_3.

^{13}C Chemical-Shift-Anisotropy Filter

To separate the signals of anomeric carbons (O-C-O) from those of aromatic carbons, both of which may resonate between 120 and 90 ppm, the aromatic-carbon signals were selectively suppressed by a five-pulse ^{13}C chemical-shift-anisotropy (CSA) filter with a CSA filter time of 35 μsec (Mao and Schmidt-Rohr, 2004). The ^{1}H 90-degree pulse-length was 4 μsec, contact time 1 msec, and CSA filter time 35 μsec. Four-pulse TOSS (Dixon, 1982) was used before detection. During detection, two-pulse phase-modulation decoupling was applied. To detect nonprotonated anomeric carbons, this filter was combined with a dipolar dephasing time of 40 μsec. Alternatively, it was also combined with short CP of 50 μsec to obtain selective spectra of protonated anomerics. The recycle delay was 0.5 sec, and the spinning speed was 6.5 kHz.

CH_2 Spectral Editing

Spectral editing of CH_2 signals was achieved by selection of the three-spin coherence of CH_2 groups, using a ^{13}C 90-degree pulse and ^{1}H 0-degree/180-degree pulses applied after the first quarter of one rotation period with MREV-8 decoupling (Mao and Schmidt-Rohr, 2005). The spinning speed was 5.787 kHz. Typically, two or three bands are observed. Nonpolar CH_2 (bonded to two carbons) is usually dominant in HA compared with other nonpolar aliphatics and resonates between 20 and 40 ppm. The NCH_2 signal often presents merely a shoulder and is between 42 and 60 ppm. The CH_2—OH group is often the second most important component and resonates between 60 and 70 ppm, whereas CH_2-O-C ethers may contribute to a signal between 68 and 75 ppm.

Long-Range Recoupled C-H Dipolar Dephasing Experiments

Fused aromatic rings typical of charcoal can be identified by their large content of carbons that are distant from protons. The signals of these carbons can be selected efficiently by a recoupled dipolar dephasing technique introduced by Mao and Schmidt-Rohr (2003). In short, two ^{1}H 180-degree pulses per rotation period prevent MAS from averaging out weak CH dipolar couplings. After 0.9 msec of recoupled dipolar dephasing time, the signals of most individual aromatic rings are dephased, whereas those of charcoal remain at the 95% level. To detect nonprotonated carbons with good relative efficiency, direct polarization (DP)/TOSS as previously described was used at a spinning speed of 7 kHz. The *γ-integral* was used to suppress sidebands up to the fourth order. The ^{13}C 90-degree and 180-degree pulse lengths were 4 μsec and 8 μsec, respectively. We examined the 4-inside-silt sample using this technique; the recycle delay was 5 sec. The dipolar dephasing times varied from 0.29 to 2.3 msec.

2D HETCOR NMR

Heteronuclear correlation (HETCOR) experiments, correlating ^{1}H and ^{13}C chemical shifts in two-dimensional spectra, were also performed. These spectra describe protons in the immediate or wider environment of a given carbon. In particular, the environments of COO/N-C=O groups can be identified, and we can determine whether aliphatic, carbohydrate, and aromatic components are in close proximity (Mao and Schmidt-Rohr, 2006; Mao et al., 2010). Lee-Goldburg cross polarization (LGCP) of 0.5-msec duration was used so that the correlations between protons and carbons separated by three or less bonds could be detected. Recycle delays were 1 sec, and 1,024 scans were averaged for each of the 96 t_1 increments.

RESULTS

Results From ^{13}C DP Compared With Results From CP/MAS NMR

Figure 1 shows the quantitative ^{13}C DP/MAS spectra of three HA from the slickspot soils 4-inside-silt, 4-inside-vesicular,

TABLE 2. Integration Results From Quantitative ^{13}C DP/MAS Spectra of an HA Fraction Extracted From Three Depths of the Slickspot Soil at Site 4

ppm	220–184	184–164	164–145	145–107	107–94	94–62	62–46	46–5
Soil layer	C=O	COO NC=O	Arom. C-O	Arom.	OCO	OCH	OCH_3 NCH	Alkyl
4-inside-silt	3	15	8	29	3	8	7	27
4-inside-vesicular	3	15	11	39	4	8	5	15
4-inside-clay	2	14	11	41	4	8	5	15

Values are percentages of total spectral area.

TABLE 3. Integration Results From Semiquantitative ^{13}C CP/TOSS Spectra of all the HA

Sample No., Location, and Soil Texture	220–184	184–164	164–145	145–107	107–94	94–62	62–46	46–5
4-inside-silt	2	11	5	21	3	15	12	31
4-inside-vesicular	2	11	8	28	4	16	10	21
4-inside-clay	2	11	8	29	4	17	10	19
4-outside-silt	3	13	7	28	3	15	12	19
4-outside-clay	2	11	7	27	3	14	11	25
5-inside-silt	2	11	5	19	2	14	13	34
5-inside-vesicular	3	10	8	26	4	17	12	20
5-inside-clay	3	9	8	27	4	17	12	20
5-outside-silt	3	12	7	25	3	14	11	25
5-outside-clay	2	12	7	27	4	16	12	20

Values are percentages of total spectral area.

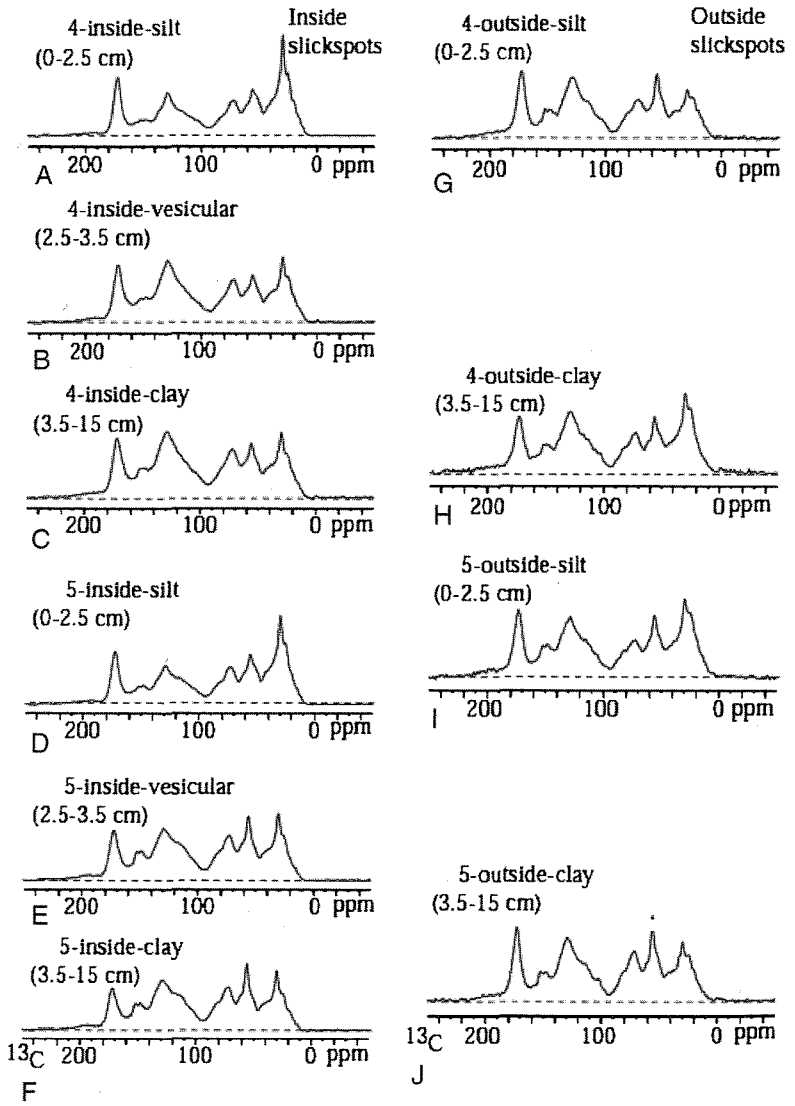

FIG. 2. Qualitative CP/TOSS/MAS ^{13}C-NMR spectra of HA from: (A) 4-inside-silt, (B) 4- inside-vesicular, (C) 4-inside-clay, (D) 5-inside-silt, (E) 5-inside-vesicular, (F) 5-inside-clay, (G) 4-outside-silt, (H) 4-outside-clay, (I) 5-outside-silt, and (J) 5-outside-clay. A total of 8k scans and 0.7-sec recycle delays for (A) to (F) and 4k scans and 0.5-sec recycle delays for (G) to (J). Spinning frequency was 6.5 kHz.

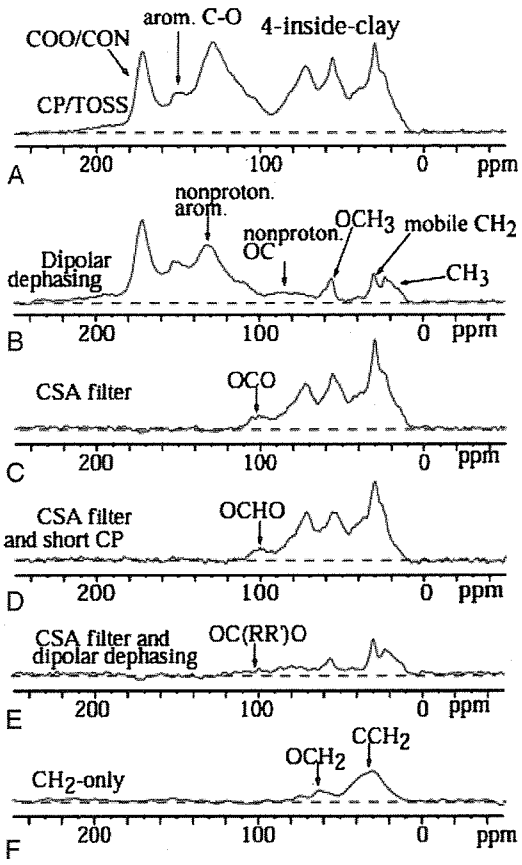

FIG. 3. Spectral editing for 4-inside-silt HA. A, Full CP/TOSS spectrum with a contact time of 1 msec, shown for reference. B, Spectrum after 40-μsec dipolar dephasing, which selects signals of nonprotonated carbons and mobile segments such as CCH_3 and OCH_3. C, Selection of alkyl carbons by a 35-μsec ^{13}C CSA filter, which in particular identifies OCO carbons resonating near 100 ppm, typical of sugar rings. D, Selection of protonated alkyl carbons by a 35-μsec ^{13}C CSA filter and short (50-μsec) CP, showing in particular OCHO signals around 100 ppm. E, Selection of nonprotonated and mobile alkyl carbons by a ^{13}C CSA filter and dipolar dephasing, which in particular identifies OC(RR')O carbons. F, Selective spectrum of CH_2 groups based on three-spin coherence selection to show CH_2 and OCH_2 bands. A total of 8k scans with 0.7-sec recycle delays were recorded for (A) to (E) and 14k scans with 0.5-sec recycle delays for (F).

and 4-inside-clay. The spectral area percentages of the relevant resonance ranges are listed in Table 2. Roughly, the assignments (Mao et al., 2000; Mao et al., 2007b) are as follows: 5 to 46 ppm, alkyl; 46 to 62 ppm, NCH and OCH_3; 62 to 94 ppm, carbohydrate C (OC); 94 to 107 ppm, O-C-O anomerics; 107 to 145 ppm, aromatic C; 145 to 164 ppm, aromatic C-O; 164 to 184 ppm, COO and N-C=O; and 184 to 220 ppm, ketone, quinone, or aldehyde C (C=O). In our samples, we observed alkyl C around 0 to 46 ppm with sharp poly(methylene) peaks at 30 ppm, OCH_3/NCH at approximately 56 ppm, OC at 72 ppm, aromatic-C at 128 ppm, aromatic C-O at ca. 150 ppm, and COO/N-C=O around 172 ppm. The spectra of 4-inside-vesicular and 4-inside-clay are quite similar, which is also reflected in the data in Table 2; there is almost no difference for the percentages of different functional groups between the two samples. In contrast, the DP spectrum of 4-inside-silt, the surface layer, contains less aromatics and aromatic C-O and almost double the content of nonpolar alkyls with a sharp poly (methylene) peak.

Figure 2 shows the semiquantitative ^{13}C CP/TOSS MAS spectra of all humic samples of Palazzo et al. (2008) to identify structural similarities or differences among the HA. Although CP is not fully quantitative, trends in HA chemical structures across soil depths and types can still be examined. Therefore, we list the spectral proportions for CP spectra (Table 3), which allows for general description of trends among samples and between CP and DP spectral proportions. A comparison of DP spectra (Fig. 1) and their corresponding CP spectra in Fig. 2 indicates that CP showed the same relative trends among depths as did DP, although CP underrepresented all forms of sp^2-hybridized carbons (C=O, COO, aromatic C-O, and aromatic C), which will be addressed later. Specifically, the CP spectra of HA from 4-inside-vesicular and 4-inside-clay were quite similar, whereas the spectrum of HA from 4-inside-silt, the surface sample, contained reduced aromatics and aromatic C-O, and more nonpolar alkyls with a very sharp poly(methylene) peak, as described in detail elsewhere (Mao et al., 2002). For the series of HA from inside slickspots at Site 5, the CP spectra show almost the same trend with increasing depth as those from inside slickspots at Site 4.

As stated by Palazzo et al. (2008), the CP spectra indicate that the HA from outside slickspots differed from those from inside slickspots in three clear aspects. First, all the HA outside slickspots exhibited significant aromatic signals, whereas the aromatics were less abundant in HA from the surface layers inside slickspots. Second, at Site 5, the HA from the surface layer, 5-outside-silt, had more nonpolar alkyls (~0–50 ppm) than did the HA from the bottom layer, 5-outside-clay. This result is consistent with the HA series from inside slickspots. However, for the two HA from outside slickspot at Site 4, the HA from the bottom clay layer contained more alkyls than those from the silt and vesicular layers. This trend is the reverse of that for HA from inside slickspots. Third, we did not observe less aromatics and aromatic C-O groups for surface layer HA from outside slickspots as in the case of inside slickspots, whereas the surface samples

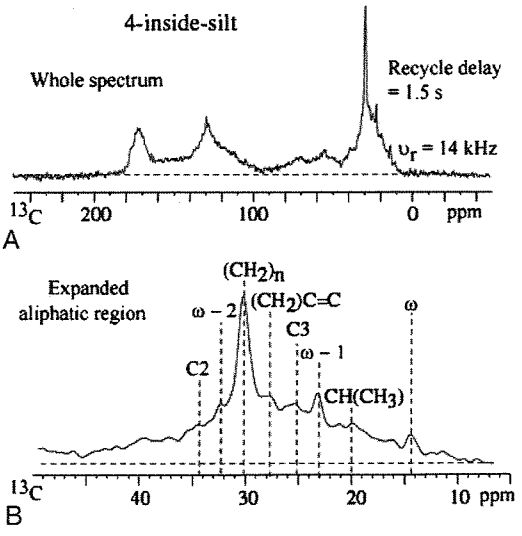

FIG. 4. Characterization of mobile aliphatic chains of HA from 4-inside silt layer by ^{13}C NMR. A, Full spectrum, obtained with ^{13}C DP/MAS and a 1.5-sec recycle delay at a spinning speed of 14 kHz. B, Expansion of the aliphatic region, with detailed assignments.

inside slickpots contained reduced aromatics and aromatic C-O groups.

Based on CP and DP spectra of three samples inside slickspots at Site 4 (Figs. 1 and 2), we can investigate the spectral differences between CP and DP. The integrals indicate that compared with the DP spectral proportions, CP consistently overestimated spectral proportions between 5 and 107 ppm, which are attributed to sp^3-hybridized carbons, and it underestimated spectral proportions between 107 and 220 ppm, which arise from sp^2-hybridized carbons (Tables 2 and 3). Specifically, averaged across the three humic fractions from Site 4, the spectral proportion that was most overestimated by CP NMR compared with DP NMR was carbohydrate C (8% overestimate), followed by OCH_3/NCH (5%) and aliphatic C (5%). Underestimation by CP NMR was greatest for aromatic-C (10% underestimate), followed by COO/NC=O and aromatic C-O (4% and 3%, respectively), and finally C=O (1%).

Functional Groups From NMR Spectral Editing

Based on the spectra in Figs. 1 and 2, we grouped the HA by their spectral features. The first category included HA from 4-inside-silt, 5-inside-silt, 5-outside-silt, and 4-outside-clay, which contained significant nonpolar alkyls but less aromatics. The second category included HA from 4-inside-vesicular, 4-inside-clay, 5-inside-vesicular, 5-inside-clay, 5-outside-clay, and 4-outside-silt, which contained less nonpolar alkyls but significant aromatics. Hence, further detailed investigations of HA chemistry were restricted to the HA from 4-inside-silt and 4- inside-clay, which are representative of the two categories.

The assignments of ^{13}C signals to specific functional groups of HA from 4-inside-clay can be clarified using spectral-editing techniques such as dipolar dephasing, ^{13}C CSA filtering combined with a short CP or dipolar dephasing, and CH_2 selection. For the 4-inside-clay sample, Fig. 3A showed the ^{13}C CP/TOSS spectrum, which displays qualitative structural information and is used primarily as a reference spectrum for the selective subspectra. The corresponding CP/TOSS spectrum after 40 μsec of dipolar dephasing (Fig. 3B) solely exhibited signals of nonprotonated carbons and mobile groups, including rotating CCH_3 groups, which have a reduced C-H dipolar coupling caused by their fast large-amplitude motion. This spectrum displays a minor peak for ketones around 184 to 220 ppm, a large peak for COO/N-C=O at ca. 172 ppm, signals for aromatic C-O around 152 ppm and nonprotonated aromatics around 128 ppm, a broad low OCq band from 65 ppm to 95 ppm, a relatively sharp OCH_3 band around 56 ppm, and signals for mobile CCH_2 around 30 ppm and for CCH_3 below 24 ppm. In addition, nonprotonated aromatic carbons in multiple oxygen-substituted rings were detected around 110 ppm. This 110-ppm band, together with the OCH_3 peak at 56 ppm and aromatic C-O around 150 ppm, is characteristic of lignin residues.

The ^{13}C CP/TOSS spectrum after a ^{13}C CSA filter of 35-μsec, which exhibits only sp^3-hybridized carbon signals, is displayed in Fig. 3C. This technique is robust in separating overlapping anomeric (O-C-O) from aromatic carbon signals between 90 and 120 ppm. Most significantly, a clear O-C-O band is displayed in this region (Fig. 3C). The combination of this filter technique with short CP (50 μsec) results in a subspectrum (Fig. 3D) of protonated sp^3-carbons. The combination of this filter technique with dipolar dephasing leads to a subspectrum (Fig. 3E) of only nonprotonated sp^3-carbons and mobile segments. Clearly, most of the O-C-O carbons are protonated because negligible nonprotonated anomerics are detected in Fig. 3E, whereas significant O-CH-O signals around 100 ppm are present in Fig. 3D. Figure 3F is the spectrum with only CH_2 signals. It clearly shows OCH_2 and CCH_2 bands around 62 ppm and 30 ppm, respectively.

Because the spectra of the group of HA represented by HA from 4-inside-silt indicate a significant fraction of nonpolar alkyls, we examined its nonpolar alkyls more closely by using ^{13}C DP/MAS with a short 1.5-sec recycle delay. A short recycle delay of 1.5 sec highlights the signal of mobile segments such as the peak around 30 ppm (Fig. 4) because the ^{13}C spin-lattice (T_1) relaxation times of highly mobile groups are shorter than those of rigid groups. Figure 4A shows the signal across the full

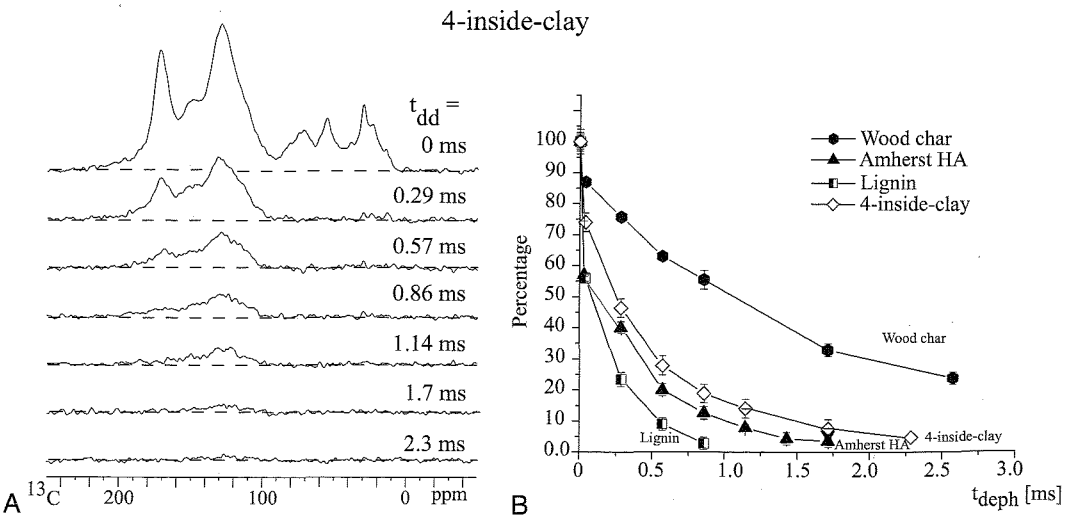

FIG. 5. A, Series of DP/TOSS spectra of HA from 4-inside-clay after recoupled dipolar dephasing of the indicated durations, ν_r = 7 kHz. Total measuring time, 35.6 h. B, Long-range dipolar dephasing curves for aromatics of 4-inside-clay HA compared with data from Mao and Schmidt-Rohr (2003) for wood charcoal, Amherst HA, and lignin. The aromatic signals were integrated between 107 and 142 ppm, which is the range expected for fused-ring carbons. The data points have been corrected slightly for regular T_2 relaxation.

spectral range. It is dominated by a large peak in the aliphatic region, plus a small COO/NC=O band around 172.4 ppm and a similarly small band around 130 ppm within the unsaturated/aromatic region, part of which could be assigned to olefinic CH=CH groups in mobile acyl chains (Mao et al., 2007b).

Figure 4B shows the expanded aliphatic region between 5 and 50 ppm of the ^{13}C DP/MAS spectrum of Fig. 4A, with detailed assignments to sites in the aliphatic chains indicated. The spectrum shows signals that are characteristic of mobile acyl chains, similar to HA from particulate organic matter in the Saguenay Fjord and the St Lawrence Estuary (Mao et al., 2007b). It displays sharp peaks of the methyl chain end (ω-carbon) at 14.2 ppm and of the two nearest methylenes (ω-1 and ω-2 carbons) at 22.9 and 32.2 ppm, respectively. On the COO end of the chain, the carbon sites C2 and C3 have chemical shifts of 34.2 and 25.1 ppm, respectively, separate from the central -$(CH_2)_n$- sites at 30.1 ppm. The adjacent CH_2CH=CH methylene groups resonate near 27.7 ppm. This result can be ascribed to a fatty acid structure with an acyl chain, as reported by Mao et al. (2007b).

Aromatic Carbons

The HA extracted from the 4-inside-clay depth contained significant amounts of aromatics. Are these aromatics composed of fused ring carbons, or instead merely single rings like lignin residues? This question can be addressed using the ^{1}H -^{13}C recoupled long-range dipolar dephasing technique (Mao and Schmidt-Rohr, 2003), which can select carbons far from protons such as are commonly found in charcoal.

Figure 5A shows a series of DP/TOSS spectra of the HA isolated from 4-inside-clay, with increasing recoupled dephasing times ranging from 0.29 to 2.3 msec. The relatively slow decay of the peaks around 128 ppm shows that recoupled long-range dipolar dephasing indeed achieved some selection of aromatics not bonded to oxygen. After a recoupled dephasing time of 2.3 msec, though, negligible signals were recorded for this sample, meaning few carbons were far removed from protons and suggesting that most aromatic carbons were not part of fused aromatic rings.

Figure 5B displays the dipolar dephasing curves of the aromatic carbons not bonded to oxygen (signal between 107 and

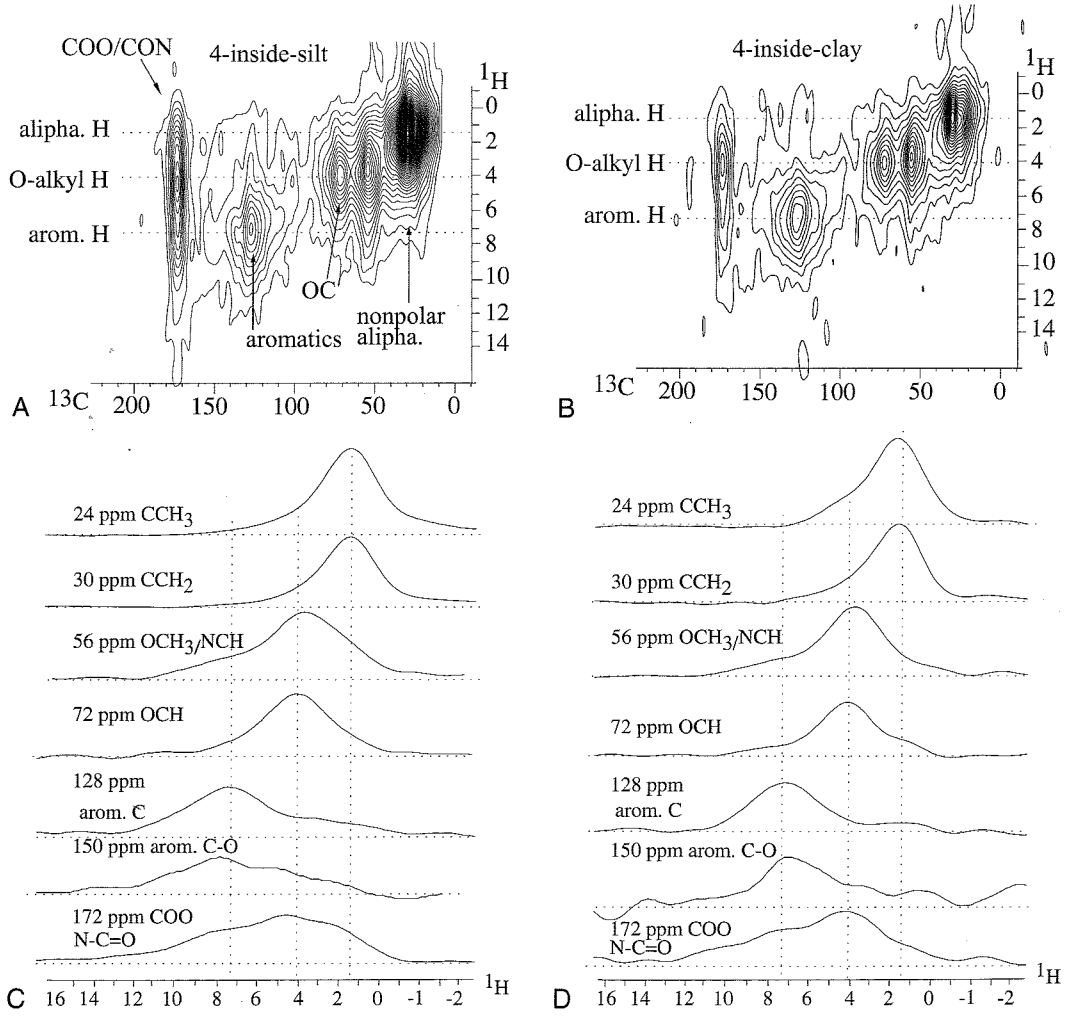

FIG. 6. Two-dimensional HETCOR with 0.5-msec LGCP spectrum of HA for (A) 4-inside-silt and (B) 4-inside-clay. Recycle delays for both spectra were 1 sec, and 1,024 scans were averaged for each of the 96 t_1 increments. The ^{1}H cross sections of the HETCOR spectra at the ^{13}C chemical shifts 24, 30, 56, 72, 128, 150, and 172 ppm for (C) 4-inside-silt and (D) 4-inside-clay.

142 ppm). To estimate the sizes of the fused aromatic rings in 4-inside-clay, we also include the dephasing curves of the Amherst HA, lignin and wood charcoal from Mao and Schmidt-Rohr (2003). The dephasing rate of 4-inside-clay is close to that of lignin and quite distinct from that of wood charcoal. Based on our previous investigations of the dephasing rates of HA and model compounds (Mao and Schmidt-Rohr, 2003), we concluded that most of the aromatics in this HA sample consist of two or three fused rings.

Structural Information From Short-Range HETCOR NMR

Correlation peaks for one- and two-bond distances were determined by ^{1}H -^{13}C HETCOR NMR with 0.5 msec of LGCP for HA from 4-inside-silt (Fig. 6A) and 4-inside-clay (Fig. 6B). The proton cross sections at the indicated ^{13}C chemical shifts were extracted to help identify the connectivities of different functional groups. For HA from 4-inside-silt, the greatest contribution to the proton cross section at the ^{13}C chemical shift of 172 ppm (COO or NC=O) was from NCH or OCH protons resonating at the ^{1}H chemical shift of 4 to 5 ppm. The contribution from HNC=O (amide) carbons, which are two bonds from the NH protons and resonate at the ^{1}H chemical shift of 8.5 ppm, was also observed. There were also signals from COOH protons, which resonate around 11 ppm or above in the ^{1}H dimension. At the ^{13}C chemical shift of 150 ppm for aromatic C-O carbons, OCH_3 protons resonating around 4 ppm contributed to a shoulder on the main peak of aromatic protons around 7 ppm. Correspondingly, the cross section at the ^{13}C chemical shift of 56 ppm displayed a shoulder at ca. 7 ppm from aromatic protons. These cross peaks indicate the presence of lignin residues. The ^{1}H cross section at the ^{13}C chemical shift of 128 ppm for aromatic C showed a shoulder that could be from alkyl H. The ^{1}H cross section at the ^{13}C chemical shift of 72 ppm for OCH showed shoulders from both alkyl and aromatic protons. The ^{1}H cross sections at the ^{13}C chemical shifts of 24 and 30 ppm (nonpolar alkyl C) were quite similar and primarily showed contributions from their own nonpolar alkyl protons.

Most of the ^{1}H slices for HA from 4-inside-clay show the same intensity pattern as the corresponding slices for HA from 4-inside-silt, except those at the ^{13}C chemical shifts of 24 ppm and 128 ppm. The ^{1}H cross section at 24 ppm in 4-inside-clay shows a more obvious shoulder above 4 ppm, indicating that CCH_2 and CCH_3 groups are more closely associated with other groups such as OCH. In the ^{1}H cross section at the ^{13}C chemical shift of 128 ppm for HA from 4-inside-silt, the shoulder in the alkyl ^{1}H region is less obvious compared with that for HA from 4-inside-clay. This suggests that aromatics in HA from 4-inside-clay are more isolated, that is, some could be from charcoal-like fused ring carbons.

Synopsis—Major Structural Units

The ^{13}C DP/MAS with a short 1.5-sec recycle delay and its expanded aliphatic region around 5 to 50 ppm allowed us to clearly identify lipid-like, mobile, long aliphatic acyl chains. Carbohydrates contribute to the signals around 60 to 90 ppm (OC) and around 90 to 120 ppm (O-C-O). Our ^{13}C CSA filter clearly demonstrated the presence of O-C-O carbons, most of which were protonated, whereas some alkyl OC carbons were nonprotonated. The ^{13}C NMR signals around 55 ppm originate from NCH and OCH_3 groups (Table 2). The dipolar-dephased spectrum indicates that both groups exist in HA from 4-inside-clay, with more NCH than OCH_3. The strong signals from NCH groups around 56 ppm and N-C=O around 173 ppm indicate the presence of peptides (O=C)-N-(C-H). The presence of both OCH_3 and nonprotonated aromatic carbons in multiple oxygen-substituted rings around 110 ppm and aromatic C-O signals is indicative of lignin residues. Fused ring carbons such as those in charcoal containing two or three aromatic rings also contribute to the aromatic signals.

Thus, we conclude that for HA represented by HA from 4-inside-silt, the major structural units are long-chain aliphatics, as well as peptides, sugar, and lignin residues. Relatively few charcoal-like aromatics are present. The same structural units are found in HA represented by HA from 4-inside-clay, but charcoal-like aromatics are more prominent and long-chain aliphatics are less abundant.

DISCUSSION

Advantages of Quantitative and Advanced Solid-State NMR Techniques Over ^{13}C CP/MAS

As previously shown (Botto et al., 1987; Nanny et al., 1997; Mao et al., 2000; Smernik et al., 2002; Keeler and Maciel, 2003; Preston et al., 2009), CP overestimates sp^3-hybridized carbons and underestimates sp^2-hybridized carbons compared with DP (Tables 2 and 3). The CP/MAS allows for up to four times more ^{13}C signal than DP/MAS (Pines, et al., 1973; Mehring, 1983; Mao et al., 2002). Moreover, the recycle delay of a CP/MAS experiment is determined by the longest ^{1}H spin-lattice relaxation time (T_1^H) of a sample, not the longest ^{13}C spin-lattice relaxation time (T_1^C) as for DP/MAS. Note that T_1^H is usually shorter than T_1^C. The CP/MAS tremendously enhances sensitivity. However, several drawbacks associated with CP, such as low CP efficiency of nonprotonated or mobile carbons, spinning sidebands, and baseline distortions, render this technique semi-quantitative (Botto et al., 1987; Nanny et al., 1997; Mao et al., 2000; Mao et al., 2002; Smernik et al., 2002; Keeler and Maciel, 2003; Mao et al., 2008; Preston et al., 2009). In our pulse sequence, we use TOSS before detection to suppress sidebands. The TOSS can also refocus magnetization before detection so as to avoid baseline distortion arising from the dead time. As shown in this study, CP/TOSS spectra are qualitatively similar to DP/MAS. Nevertheless, because of their larger chemical shift anisotropy, the sp^2 carbon signal is less completely refocused than sp_3 hybridized C during TOSS, and therefore CP/TOSS underestimated sp^2-hybridized and overestimated sp^3-hybridized carbons compared with DP/MAS.

The DP/MAS provides quantitative structural information by using direct polarization and avoiding CP and thus the problems associated with CP. But the sensitivity of the DP experiments is greatly reduced without CP. Therefore, many more scans are required to acquire a reasonably good-quality DP spectrum compared with CP.

Traditional ^{13}C CP/MAS and DP/MAS spectra of SOM have broad peaks because SOM is a heterogeneous and complex mixture. It can be difficult to identify certain functional groups. For example, around 90 to 120 ppm for a typical ^{13}C SOM spectrum, sp^3-hybridized anomerics and sp^2-hybridized aromatics overlap. To overcome this problem, spectral-editing techniques that select specific functional groups are needed. As shown in Fig. 3, the spectral-editing techniques allowed the selection of nonprotonated carbons and mobile groups, alkyl carbons, CH, and CH_2 groups which would otherwise be buried in the heavily overlapped broad spectrum. In addition, ^{1}H-^{13}C two-dimensional HETCOR can provide connectivities and proximities of specific functional groups, and ^{1}H-^{13}C recoupled long-range dipolar dephasing can allow the identification and estimation of the sizes of fused-ring carbons. Thus, advanced solid-state NMR

techniques promise to provide more structural information than ^{13}C CP/MAS and ^{13}C DP NMR alone.

Variation of HA Chemical Structures With Depth

Various measurements of HA characteristics for the slickspot soils indicated an increasing degree of humification with increasing soil depth from the silt layer to the vesicular and clay layers. The elemental compositions previously reported (Palazzo et al., 2008) suggested this trend because C, N, and H concentrations typically decrease and O concentration typically increases with humification through microbially driven oxidation processes. Similarly, ^{13}C-NMR spectra showed that for all soils, except those from outside slickspots at Site 4, the HA from the deeper vesicular and clay layers contain less nonpolar alkyls and more aromatics compared with those from surface silt layers. Such a relative enrichment of aromatic C was identified by Zech et al. (1997) as a key feature of increasing humification. A relative enrichment of aromatics and depletion of nonpolar alkyls with depth was also reported by Schmidt et al. (2000) for a forest Podzol soil in Germany and by Stearman et al. (1989) for crop soils in the United States. Asakawa et al. (2007) also found that a hydrophobic fraction of SOM became enriched with aromatics at increasing depth for a forest soil in Japan, but its alkyl C content did not decrease with depth. Carboxyl groups are also thought to increase with humification, and accordingly, Gondar et al. (2005) and Lopez et al. (2008) reported an enrichment of carboxyls with soil depth. In addition, the reductions in carbohydrates with soil depth were observed (Beyer et al., 1995; Gressel et al., 1995; and Enloe et al., 2010). We speculate that organic matter at depth might be relatively enriched in humified materials such as aromatic C and carboxyls compared with the surface horizon because of smaller and less regular input of fresh plant material to these depths, as was hypothesized earlier by Stearman et al. (1989) for crop soils.

In addition to soil depth, the differences in HA chemistry among the uppermost silt layer, intermediate vesicular layer, and underlying clay layer might also be attributable to differences in their respective textures or structures. However, according to studies using NMR and other analytical procedures as reviewed by Schulten and Leinweber (2000) and Christensen (1992), clay-sized particles tend to have greater proportions of alkyl-C and smaller proportions of aromatic C than do silt-sized and sand-sized particles. Silt-sized particles tend to have the greatest proportions of aromatic C. These trends contradict our results. Hence, we conclude that soil depth was the primary factor controlling HA chemistry in the silt, vesicular, and clay layers.

Variations of HA Chemical Structures Inside and Outside Slickspots

The limited number of samples analyzed allows only a few comparisons for the structural components of HA inside and outside slickspots. The HA from the surface silt layer contained larger proportions of aromatics outside the slickspots than inside the slickspots, whereas the aromatic proportions of HA from the vesicular and clay layers did not differ between inside and outside the slickspot. Inside the slickspots, the HA from the silt layers contained less aromatics than those from vesicular and clay layers. A key objective of this study was to identify any differences in HA chemistry between the inside-slickspot soils and the outside soils. The single notable difference in HA chemistry was a smaller proportion of aromatic C in HA from the surface silt layer of the slickspot compared with the surface silt layer of the outside soil (Fig. 2). Time and financial constraints limited the number of samples that were analyzed in this study. Further work would be needed to relate this finding to soil processes in this saline soil. For example, Loffredo et al. (2010) evaluated the germination and establishment of peppergrass on slickspot soils.

CONCLUSIONS

Our advanced solid-state NMR techniques enabled a detailed characterization of HA from slickspots. All HA are composed of five major structural components: aliphatic chains, peptides, sugar rings, lignin residues, and aromatic/olefinic carbons. Advanced ^{13}C-NMR spectra showed that for all soils, except those outside slickspots at Site 4, the HA from the deeper vesicular and clay layers contained less nonpolar alkyls and more aromatics than did those from surface silt layers. Furthermore, the HA from the outside layers contained relatively large proportions of aromatics, similar to the HA from vesicular and clay layers both inside and outside the slickspots. Inside the slickspots, the HA from the top silt layers had a lower aromaticity than those from vesicular and clay layers. These results do not identify any chemical characteristic of the HA from the slickspot soils that would clearly inhibit or promote plant growth. Our advanced solid-state NMR techniques promise to provide more structural information than ^{13}C CP/MAS and ^{13}C DP NMR can achieve. Compared with DP, CP overestimated spectral proportions of sp^3-hybridized carbons and underestimated spectral proportions of sp^2-hybridized carbons.

ACKNOWLEDGMENTS

This work was supported by the National Science Foundation (EAR-0843996 and CBET-0853950), the Thomas F. Jeffress and Kate Miller Jeffress Memorial Trust, and by the Airspace, Ranges, and Airfield Operations Division, HQ Air Combat Command, Langley AFB, VA. The opinions and conclusions in this article are those of the authors and do not necessarily reflect those of the U.S. Air Force, U.S. Army, or the federal government. The authors also thank Prof. Klaus Schmidt-Rohr for his kind support.

REFERENCES

Asakawa, D. D., H. Mochizuki, Y. Yanagi, and N. Fujitake. 2007. Characterization of hydrophobic acid fractions in water-soluble organic matter in Dystric Cambisol and in a stream in a small forested watershed: Seasonal and vertical variations in chemical properties. Soil Sci. Plant Nutr. 53:551–561.

Beyer, L., C. Sorge, H. P. Blume, and H. R. Schulten. 1995. Soil organic matter composition and transformation in Gelic Histosols of coastal continental Antarctica. Soil Biol. Biochem. 27:1279–1288.

Botto, R. E., R. Wilson, and R. E. Winans. 1987. Evaluation of the reliability of solid ^{13}C NMR spectroscopy for the quantitative analyses of coals: Study of whole coals and maceral concentrates. Energy Fuels 1:173–181.

Christensen, B. 1992. Physical fractionation of soil and organic matter in primary particle size and density separates. Adv. Soil Sci. 20:1–90.

Dixon, W. T. 1982. NMR spectra in spinning sidebands (TOSS). J. Chem. Phys. 77:1800–1809.

Enloe, H. A., S. A. Quideau, R. C. Graham, S. C. Sillett, S. W. Oh, and R. E. Wasylishen. 2010. Soil organic matter processes in old-growth redwood forest canopies. Soil Sci. Soc. Am. J. 74:161–171.

Fisher, H., L. Eslick, and M. Seyfried. 1996. Edaphic Factors That Characterize the Distribution of *Lepidium papilliferum*. Idaho Bureau of Land Management, Idaho State Office, Technical Bulletin 96-6, Boise, Idaho.

Gondar, D., R. López, S. Fiol, J. M. Antelo, and F. Arce. 2005. Effect of soil depth on acid properties of humic substances extracted from an ombrotrophic peat bog in northwest Spain. Eur. J. Soil Sci. 56:793–801.

Gressel, N., Y. Inbar, A. Singer, and Y. Chen. 1995. Chemical and spectroscopic properties of leaf litter and decomposed organic matter in the Carmel Range, Israel. Soil Biol. Biochem. 27:23–31.

Harkness, A. L. 1998. Soil Survey of Owyhee County Area, Idaho. U.S. Department of Agriculture, Soil Conservation Service, Boise, Idaho.

Jones, J. B. Jr. 1999. Soil Analysis Handbook of Reference Methods. Soil and Plant Analysis Council, CRC Press, Boca Raton, FL.

Hatcher, P. G., K. J. Dria, S. Kim, and S. W. Frazier. 2001. Modern analytical studies of humic substances. Soil Sci. 166:770–794.

Keeler, C., and G. E. Maciel. 2003. Quantitation in the solid-state C-13 NMR analysis of soil and organic soil fractions. Anal. Chem. 75: 2421–2432.

Lewis, G. C., J. V. Jordan, and M. A. Fosberg. 1959. Tracing moisture movement in slick- spot soils with radiosulfur, Part II. Soil Sci. Soc. Am. Proc. 23:206–210.

Lewis, G. C., and J. L. White. 1964. Chemical and mineralogical studies on slick spot soils in Idaho. Soil Sci. Soc. Proc. 28:805–808.

Li, X.-G., F.-M. Li, Q.-F. Ma, and Z.-J. Cui. 2006. Interactions of NaCl and Na_2SO_4 on soil organic C mineralization after addition of maize straws. Soil Biol. Biochem. 38:2328–2335.

Loffredo, E., A. J. Palazzo, N. Senesi, C. E. Clapp, and T. L. Bashore. 2010. Germination and early growth of slickspot peppergrass (*Lepidium papilliferum*) as affected by desert soil humic acids. Soil Sci. 175: 186–193.

Lopez, R., D. Gondar, A. Iglesias, S. Fiol, J. Antelo, and F. Arce. 2008. Acid properties of fulvic and humic acids isolated from two acid forest soils under different vegetation cover and soil depth. Eur. J. Soil Sci. 59: 892–899.

Luna-Guido, M. L., R. I. Beltrán-Hernández, and L. Dendooven. 2001. Dynamics of ^{14}C-labelled glucose in alkaline saline soil. Soil Biol. Biochem. 33:707–719.

Mathers, N. J., X. A. Mao, Z. H. Xu, P. G. Saffigna, S. J. Berners-Price, and M. C. S. Perera. 2000. Recent advances in the application of C-13 and N-15 NMR spectroscopy to soil organic matter studies. Aus. J. Soil Res. 38:769–787.

Mao, J.-D., W.-G. Hu, K. Schmidt-Rohr, G. Davies, E. A. Ghabbour, and B. Xing. 2000. Quantitative characterization of humic substances by solid-state carbon-13 nuclear magnetic resonance. Soil Sci. Soc. Am. J. 64:873–884.

Mao, J.-D., L. S. Hundal, M. L. Thompson, and K. Schmidt-Rohr. 2002. Correlation of poly(methylene)-rich aliphatic domains in humic substances with sorption of a nonpolar organic contaminant, phenanthrene. Environ. Sci. Technol. 36:929–936.

Mao, J.-D., and K. Schmidt-Rohr. 2003. Recoupled long-range C-H dipolar dephasing in solid- state NMR, and its use for spectral selection of fused aromatic rings. J. Magn. Reson. 162:217–227.

Mao, J.-D., and K. Schmidt-Rohr. 2004. Separation of aromatic-carbon ^{13}C NMR signals from di-oxygenated alkyl bands by a chemical-shift-anisotropy filter. Solid State Nucl. Magn. Reson. 26:36–45.

Mao, J.-D., and K. Schmidt-Rohr. 2005. Methylene spectral editing in solid-state NMR by three- spin coherence selection. J. Magn. Reson. 176:1–6.

Mao, J.-D., and K. Schmidt-Rohr. 2006. Absence of mobile carbohydrate domains in dry humic substances proven by NMR, and implications for organic-contaminant sorption models. Environ. Sci. Technol. 40: 1751–1756.

Mao, J.-D., R. M. Cory, D. M. McKnight, and K. Schmidt-Rohr. 2007a. Characterization of a nitrogen-rich fulvic acid and its precursor algae by solid-state NMR. Org. Geochem. 38:1277–1292.

Mao, J.-D., L. Tremblay, J. P. Gagné, S. Kohl, J. Rice, and K. Schmidt-Rohr. 2007b. Humic acids from particulate organic matter in the Saguenay Fjord and the St. Lawrence Estuary investigated by advanced solid-state NMR. Geochim. Cosmochim. Acta. 71:5483–5499.

Mao, J.-D., D. C. Olk, X. W. Fang, Z. Q. He, and K. Schmidt-Rohr. 2008. Influence of animal manure application on the chemical structures of soil organic matter as investigated by advanced solid-state NMR and FT-IR spectroscopy. Geoderma 146:353–362.

Mao, J.-D., A. Schimmelmann, M. Mastalerz, P. G. Hatcher, and Y. Li. 2010. Structural features of a bituminous coal and their changes during low-temperature oxidation and loss of volatiles investigated by advanced solid-state NMR spectroscopy. Energy Fuels 24:2536–2544.

Mehring, M. 1983. High Resolution NMR in Solids. Springer, Berlin, Germany.

Nelson, P. N., J. N. Ladd, and J. M. Oades. 1996. Decomposition of ^{14}C-labelled plant material in a salt-affected soil. Soil Biol. Biochem. 28: 433–441.

Nanny, M. A., R. A. Minear, and J. A. Leenheer. 1997. Nuclear Magnetic Resonance in Environmental Chemistry. Oxford University Press, New York, NY.

Palazzo, A. J., C. E. Clapp, N. Senesi, M. H. B. Hayes, T. J. Cary, J.-D. Mao, and T. J. Bashore. 2008. Isolation and characterization of humic acids in Idaho slickspot soils. Soil Sci. 173:375–386.

Pines, A., M. G. Gibby, and J. S. Waugh. 1973. Proton-enhanced NMR of dilute spins in solids. J. Chem. Phys. 59:569–590.

Preston, C. M. 1996. Applications of NMR to soil organic matter analysis: History and prospects. Soil Sci. 161:144–166.

Preston, C. M., J. R. Nault, and J. A. Trofymow. 2009. Chemical changes during 6 years of decomposition of 11 litters in some Canadian forest sites. Part 2. C-13 abundance, solid-state C-13 NMR spectroscopy and the meaning of "lignin." Ecosystems 12:1078–1102.

Rasmussen, W. W., D. P. Moore, and L. A. Alban. 1972. Improvement of a solonetzic (slick spot) soil by deep plowing, subsoiling, and amendments. Soil Sci. Soc. Am. J. 36:137–142.

Reid, D. A., R. C. Graham, R. J. Southard, and C. Amrhein. 1993. Slickspot soil genesis in the Carrizo Plain, California. Soil Sci. Soc. Am. J. 57: 162–168.

Sandoval, F. M. Jr, M. A. Fosberg, and G. C. Lewis. 1959. A characterization of the Sebree-Chilcott Soil series association (slick spots) in Idaho. Soil Sci. Soc. Am. J. 23:317–321.

Schmidt, M. W. I., H. Knicker, and I. Kögel-Knabner. 2000. Organic matter accumulating in Aeh and Bh horizons of a Podzol—Chemical characterization in primary organo-mineral associations. Org. Geochem. 31: 727–734.

Schulten, H.-R., and P. Leinweber. 2000. New insights into organic-mineral particles: composition, properties and models of molecular structure. Biol. Fertil. Soils 30:399–432.

Smernik, R. J., J. A. Baldock, and J. M. Oades. 2002. Impact of remote protonation on ^{13}C CPMAS NMR quantitation of charred and uncharred wood. Solid State Nucl. Magn. Reson. 22:71–82.

Stearman, G. K., R. J. Lewis, L. J. Tortorelli, and D. D. Tyler. 1989. Characterization of humic acid from no-tilled and tilled soils using carbon-13 nuclear magnetic resonance. Soil Sci. Soc. Am. J. 53:744–749.

Swift, R. S. 1996. Organic matter characterization. *In*: Methods of Soil Analysis, Part 3: Chemical Methods, SSSA Book Series No. 5. D. L. Sparks (ed.). SSSA and ASA, Madison, WI, pp. 1011–1069.

Wong, V. N. L., R. C. Dalal, and R. S. B. Greene. 2008. Salinity and sodicity effects on respiration and microbial biomass of soil. Biol. Fertil. Soils 44:943–953.

Zech, W., N. Senesi, G. Guggenberger, K. Kaiser, J. Lehmann, T. M. Miano, A. Miltner, and G. Schroth. 1997. Factors controlling humification and mineralization of soil organic matter in the tropics. Geoderma 79: 117–161.